Progress in Crystal Growth and Characterization of Materials 58 (2012) 61–73

Contents lists available at SciVerse ScienceDirect

Progress in Crystal Growth and Characterization of Materials

journal homepage: www.elsevier.com/locate/pcrysgrow

Modeling on ammonothermal growth of GaN semiconductor crystals

Qi-Sheng Chen*, Jun-Yi Yan, Yan-Ni Jiang, Wei Li

Institute of Mechanics, Chinese Academy of Sciences, 15 Bei Si Huan Xi Road, Beijing 100190, China

Keywords:
GaN crystal
Baffle opening
Ammonothermal growth
Mass transfer

A B S T R A C T

Ammonothermal systems are modeled using fluid dynamics and heat and mass transfer models. The nutrient is considered as a porous media bed and the flow is simulated using the Darcy–Brinkman–Forchheimer model. The resulting governing equations are solved using the finite volume method. The effects of baffle design on flow pattern, heat and mass transfer in an autoclave are analyzed. For the research-grade autoclave with an internal diameter of 2.22 cm, the constraint for the GaN growth is found to be the growth kinetics and the total area of seed surfaces in the case of baffle opening of 10% (including the central opening of 5% and ring opening of 5%). The fluid flow across the baffle is a clockwise circulating flow which goes upwards in the central hole and downwards in the ring gap. Transport phenomena have been also studied in large-size ammonothermal growth systems with internal diameters of 4.44 cm and 10 cm. The flow pattern across the baffle changes to an anticlockwise circulating flow which goes upwards in the ring gap and downwards in the central hole in the case of 10% baffle opening. Since ammonothermal growth experiments are expensive and time-consuming, modeling becomes an effective tool for research and optimization of the ammonothermal growth processes.

1. Introduction

Gallium nitride (GaN) is a wide-bandgap semiconductor with a wide array of applications in optoelectronics and electronics. GaN-devices have gained a rapid development in the last ten years

* Corresponding author. Tel.: +86 10 82544092.
E-mail address: qschen@imech.ac.cn (Q.-S. Chen).

0960-8974/$ – see front matter © 2012 Elsevier Ltd. All rights reserved.
doi:10.1016/j.pcrysgrow.2012.02.005

since the major technological hurdles were overcome in the early 1990s. The similarity of ammonia and water as polar solvents allows GaN crystals to grow in ammonia solvents in the same way as in the hydrothermal growth of oxides crystals in high-pressure water solutions.

The ammonothermal growth of 1-inch size (0001) GaN crystal in a cylindrical high-pressure autoclave with an internal diameter of 40 mm was reported by Hashimoto et al. [1–3]. Basic mineralizers were used to obtain a retrograde solubility of GaN in supercritical ammonobasic solutions. The nutrient was placed in the colder region (upper region) and free-standing c-plane HVPE-GaN seed crystals were placed in the hotter region (lower region). Temperatures on the outer surface of the autoclave were set at 675 °C for the lower zone and 625 °C for the upper zone, and the pressure was about 214 MPa. Metallic Ga was used as a nutrient, and 1 M $NaNH_2$ and 0.05 M NaI were used as mineralizers. About 15-μm-thick GaN films were uniformly grown on each side of the seed. The growth rate is about 0.02 mm/day. The Ga-polar surface was filled with pits whereas the N-polar surface was featureless. The photoluminescence (PL) characterization also indicated qualitatively uniform optical properties on each side of the crystal.

D'Evelyn et al. [4] gave an overview of the high-pressure ammonothermal method, which is based on adaptation of high-pressure apparatus developed for diamond growth. They described recent progress in reductions of impurity concentrations, wafering and fabrication of homoepitaxial laser diodes on substrates. Crystals were grown at temperatures between 600 and 1000 °C at liquid ammonia fills of about 70–95% in volume. The pressure is estimated as lying between about 5 and 200 MPa.

Bockowski et al. [5] carried out high-pressure solution growth of GaN on HVPE seeds in a reactor with an internal diameter of 10 cm, working up to 1 GPa. A multizone graphite furnace working up to 2000 K was used. The temperatures were 1623 K and 1673 K for the upper and lower parts of the autoclave and the N_2 pressure of 0.75 GPa was generated in the reactor. The average growth rate on c planes was about 0.16 mm/day during a period of 40–200 h.

Ketchum and Kolis [6] grew ammonothermal single crystals of gallium nitride in supercritical ammonia at 400 °C and 2.4 kbar by using potassium amide (KNH_2) and potassium iodide (KI) as mineralizers. Hexagonal GaN crystal of $0.5 \times 0.2 \times 0.1$ mm^3 was obtained. Callahan et al. [7] found that the solubility of GaN in supercritical ammonia solutions in the presence of alkali amide mineralizers decreases with increasing temperatures. GaN solubility from 1% to 14% in weight was obtained in 2–4 M amide ammonia solutions. Little GaN formation was evident when growth temperatures are below 400 °C, suggesting the temperatures for the seeded growth of GaN in autoclaves are between 400 and 600 °C. Wang et al. [8,9] demonstrated single crystals of $10 \times 10 \times 1$ mm^3 in size grown under the conditions of 475–625 °C and 100–300 MPa. A growth rate up to 2 mm/day was achieved. When using basic mineralizers, the Ni contributes to the impurities at the interface between the grown GaN crystal and the seed. Also, Ni seems to act as a catalyst for GaN and therefore direct contact with the solution should be avoided. The use of basic mineralizers under the conditions of supercritical ammonia causes the retrograde solubility of GaN, e.g., a lightly increased temperature in the GaN growth zone is required to initiate the nucleation. GaN has a negative solubility coefficient and rather high solubility (1–10%) in KNH_2–NH_3 solutions between 400 and 600 °C when pressure is between 120 and 240 MPa. More details on the ammonothermal growth of GaN crystals can be found in [10].

Dwilinski et al. [11] were among the first to synthesize AlN and GaN microcrystals ammonothermally. GaN-containing feedstock was dissolved in a supercritical ammonia solution in one zone of the high-pressure autoclave, then transported through solution by means of convection, and finally crystallized in the second zone, preferably on GaN seeds. The typical temperatures and pressures applied are 0.1–0.3 GPa and 500 °C–900 °C, respectively. The crucial point is the choice of mineralizer – the ionic substance added to the reaction zone in order to increase a dissolution of GaN in ammonia. Dwilinski at al. [12,13] grew 1-in GaN crystals by using basic mineralizers. The basic mineralizers provide a non-destructive environment to the autoclave materials (Ni–Cr alloys) as contract to the acidic mineralizers which require use of Pt-liners. GaN crystals obtained using basic mineralizers are of pure hexagonal phase. The solubilities of GaN in the $NH_3 + KNH_2$ solution with molar ratio KNH_2:$NH_3 = 0.07$ were measured as a function of pressure at two temperatures 400 and 500 °C. The maximum solubility of GaN is about 3 mol%. In the ammonothermal method of growing bulk GaN single crystals, developed by the AMMONO company in collaboration with Nichia Corporation

(AMMONO-Bulk method), the growth is carried out in so called ammonobasic regime, where the mineralizer introduces $NH2^{-1}$ ions to the solution. As a consequence, the chemical transport of GaN is directed from the low temperature zone of the autoclave to the high temperature zone. As convection is a driving force for the mass transport, one has to place the high temperature zone (with seeds) below the low temperature zone (with feedstock) in order to obtain an efficient recrystallization.

Yoshikawa et al. [14] grew GaN crystal by the ammonothermal method using Ga metal precursor, supercritical ammonia solution and NH_4Cl mineralizer. Reaction was carried out with supercritical ammonia at the temperature of 500 °C and pressure of 135 MPa. Inner wall of autoclave is covered with Pt so as to prevent possible contamination from autoclave. Needle-shaped and hexagonal-shaped GaN could be grown. Using Ga metal as precursor can result in production of H_2 gas. Recrystallization of GaN from Ga metal was also confirmed under the condition of 500 °C and 120 MPa, which was the lowest reaction pressure ever reported for GaN growth by the ammonothermal method.

Using acidic mineralizers such as 0.4 M NH_4Cl, GaN has a normal solubility in ammonia [15]. The acidic conditions required the use of a Pt inner liner to protect the autoclave from corrosion. Kagamitani et al. [15] grew 0.1-mm thick GaN on a 10-mm HVPE seed in an autoclave of 16-mm inner diameter over a period of 10 days. A growth rate of 0.02–0.03 mm/day can be achieved at a temperature of 550 °C and a pressure of less than 150 MPa. Ehrentraut et al. [16] recent research aimed at optimizing the mineralizer to achieve a high yield of the hexagonal GaN phase. Fukuda and Ehrentraut [17–19] grew 0.5-mm-thick GaN on a 1-in HVPE seed at a growth temperature of about 500 °C and a pressure less than 130 MPa. The growth rate is about 0.04 mm/day. Ehrentraut et al. [20] reviewed the development in the acid ammonothermal crystal growth of GaN. They grew 0.5-mm-thick GaN on the 2-in HVPE-GaN seed in an autoclave of 100-mm inner diameter. The growth temperatures were 425 °C/525 °C for the upper/lower zones and pressure was 145 MPa. They estimated that the growth rate can reach about 1 mm/day for 1 mol% mineralizer of NH_4Cl in NH_3, when the solubility of GaN is about 20 mol% in NH_3.

Hashimoto et al. [21] reported on improvement in the structural quality of GaN grown by the ammonothermal method. The threading dislocation densities estimated by plan-view transmission electron microscopy (TEM) observations were less than 1×10^6 cm^{-2} for the Ga face and 1×10^7 cm^{-2} for the N face. The grown crystal showed anisotropy of growth rate; the thickest part was along the m direction (300 μm), followed by the $-c$ direction (180 μm) and the $+c$ direction (40 μm). No dislocation generation at the interface was observed on the Ga face, although a few defects were generated at the interface on the N face. The improvement in the structural quality, together with the growth rate and scalability, demonstrates the commercial feasibility of the ammonothermal GaN growth.

Chen et al. [22] studied the effects of particle size on flow pattern and temperature distribution in the autoclave. The autoclave used has an internal diameter of 0.932 cm, external diameter of 3.5 cm (Tem-Press MRA 138R with a volume of 12.5 ml). Chen et al. [23] modeled the GaN growth process in an autoclave with an internal diameter of 2.22 cm, external diameter of 7.62 cm (Tem-Press MRA 378R with a volume of 134 ml). Numerical studies were also performed for an ammonothermal system with a retrograde solubility [24]. The charge of 10.1 cm in height is put 2.5 cm above the baffle. In the following, the effect of baffle design on the fluid flow and heat and mass transfer will be studied.

2. Physical and mathematical models

The ammonothermal growth process uses ammonia solvents under high temperatures and high pressures to dissolve and recrystallize reagents. After the system is pressurized, solvent such as ammonia occupies most of the volume. The convection system for ammonothermal growth consists of a porous bed whose height changes with the growth, a fluid layer overlying this porous bed, a metal baffle with holes which lies above the porous bed, and a solid seed plates whose size increase with the growth. Fig. 1 shows the schematic of a growth system that has been used to synthesize GaN. The autoclave has an internal diameter of 2.22 cm, external diameter of 7.62 cm, internal height of 35.56 cm and external height of 38.10 cm (Tem-Press MRA 378R with a volume of 134 ml). The thickness of the sidewall of the autoclave is 2.54 cm. The baffle is located at a distance of 15.24 cm from the bottom of the autoclave. A baffle made from 0.28 mm Ag foil is used to divide the autoclave into two parts - upper and lower portions.

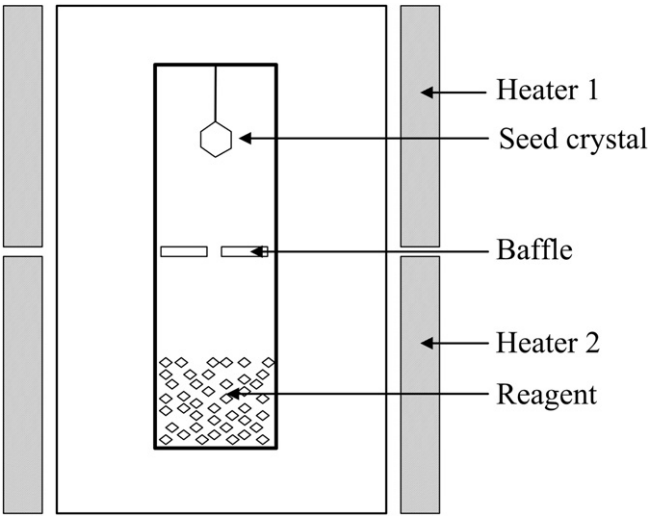

Fig. 1. Schematic of an ammonothermal growth system.

Hence the upper portion can be considered as a fluid layer with the assumption of incompressible flow and the Boussinesq approximation [25,26], and the Navier–Stokes equations can be used in the fluid layer. Suppose the density has a linear temperature dependence of the form $\rho = \rho_0[1 - \beta(T - T_0)]$, where ρ, T, and β are density, temperature, and isobaric coefficient of expansion, and ρ_0 and T_0 are constant reference values for the density and temperature, respectively. In the solid region which comprises of the autoclave walls, the baffle and the seeds, only conductive heat transfer is considered. In the fluid region, convective heat transfer is considered.

The nutrient particles of GaN in the bottom of the autoclave can be considered as a porous medium. In this case, the Darcy–Brinkman–Forchheimer model can be employed in the porous layer. The dimensionless parameters of the system are listed as follows:

$$A = H/R,\ Gr = g\beta R^3\Delta T/\nu^2,\ \mathrm{Pr} = \nu/\alpha,\ Sc = \nu/D,\ Da = K/R^2,\ Fs = b/R,$$

where A, *Gr*, *Pr*, *Sc*, *Da*, *Fs* denote aspect ratio, Grashof number, Prandtl number, Schmidt, Darcy number, and Forchheimer number, respectively. H is the internal height of the autoclave, R is the internal radius of the autoclave, g is acceleration due to gravity, ΔT is the maximum temperature difference on the sidewall of the autoclave, ν is kinematic viscosity, α is thermal diffusivity, D is the mass diffusivity, the permeability of porous matrix $K = d_p^2\varepsilon^3/\left(150(1-\varepsilon)^2\right)$ with d_p as the average diameter of the nutrient particles, and the Forchheimer coefficient $b = 1.75/\left(\sqrt{150}\varepsilon^{1.5}\right)K^{0.5}$

The governing equations in the porous and fluid layers can be combined by defining a binary parameter B as: $B = 0$ in the fluid layer and $B = 1$ in the porous layer, respectively. The porosity $\varepsilon = 0$ in solid, $0 < \varepsilon < 1$ in porous layer and $\varepsilon = 1$ in fluid layer, respectively. The combined governing equations in a cylindrical coordinate system are:

$$\frac{\partial\left(\varepsilon\rho_f\right)}{\partial t} + \nabla\cdot\left(\rho_f\mathbf{u}\right) = 0, \tag{1}$$

$$\frac{\rho_f}{\varepsilon}\frac{\partial\mathbf{u}}{\partial t} + \frac{\rho_f}{\varepsilon}(\mathbf{u}\cdot\nabla)\frac{\mathbf{u}}{\varepsilon} = -\nabla p - \rho_f\beta(T - T_0)\mathbf{g} + \nabla\cdot(\mu_e\nabla\mathbf{u}) - B\left[\left(\frac{\mu_f}{K} + \frac{\rho_f b}{K}|\mathbf{u}|\right)\mathbf{u}\right], \tag{2}$$

$$(\rho c_p)_e \frac{\partial T}{\partial t} + (\rho c_p)_f [(\mathbf{u}\cdot\nabla)T] = \nabla\cdot(k_e \nabla T), \tag{3}$$

$$\frac{\partial}{\partial t}(\rho_e C) + \nabla\cdot(\rho_e \mathbf{u} C) = \rho_e D_e \nabla^2 C - B\rho_e k_g \beta_s \varepsilon (C - C_0), \tag{4}$$

where μ, k, c_p denote dynamic viscosity, thermal conductivity, and specific heat, respectively. g is the gravity vector, k_g is the mass transfer coefficient for crystal growth from solution at the growth interface. β_s is the surface-area-to-volume ratio. Subscript f, e denote fluid and effective, respectively. The reaction and the growth rate expression at the growth interface are as follows:

$$GaN + (x-3)NH_3 + 2NH_3 \leftrightarrow Ga(NH_2)_X$$

$$v_c = \frac{D_e}{\left(\rho_S - \rho_f c\right)} \frac{\partial\left(\rho_f c\right)}{\partial n} = k_g(c_i - c_0) \text{ where}$$

$$k_g \approx 10^{-6}\ m/s$$

The following scales are used to non-dimensionalize the governing equations: length R; velocity, $u_0 = \nu/R$; time, $t_0 = R^2/\nu$; pressure, $\rho\nu^2/R^2$; and temperature, $T_H - T_L$. T_H and T_L are the high temperature and low temperature applied on the sidewall of the autoclave, respectively. The resulting non-dimensionalized equations are,

$$\frac{\partial \varepsilon\overline{\rho}}{\partial t} + \frac{1}{r}\frac{\partial}{\partial r}(r\overline{\rho}u) + \frac{\partial}{\partial z}(\overline{\rho}w) = 0, \tag{5}$$

,

$$\begin{aligned}\frac{\partial}{\partial t}\left(\frac{1}{\varepsilon}\overline{\rho}u\right) + \frac{1}{r}\frac{\partial}{\partial r}\left(\frac{1}{\varepsilon^2}r\overline{\rho}uu\right) + \frac{\partial}{\partial z}\left(\frac{1}{\varepsilon^2}\overline{\rho}wu\right) &= \overline{\mu}\left[\frac{1}{r}\frac{\partial}{\partial r}\left(r\frac{\partial u}{\partial r}\right) + \frac{\partial^2 u}{\partial z^2} - \frac{u}{r^2}\right] \\ &- \frac{\partial p}{\partial r} - B\left(\frac{1}{\mathrm{Re}Da} + \frac{Fs}{Da}|\mathbf{u}|\right)\overline{\rho}u,\end{aligned} \tag{6}$$

$$\begin{aligned}\frac{\partial}{\partial t}\left(\frac{1}{\varepsilon}\overline{\rho}w\right) + \frac{1}{r}\frac{\partial}{\partial r}\left(\frac{1}{\varepsilon^2}r\overline{\rho}uw\right) + \frac{\partial}{\partial z}\left(\frac{1}{\varepsilon^2}\overline{\rho}ww\right) &= \overline{\mu}\left[\frac{1}{r}\frac{\partial}{\partial r}\left(r\frac{\partial w}{\partial r}\right) + \frac{\partial^2 w}{\partial z^2}\right] \\ &- \frac{\partial p}{\partial z} + Gr\Theta - B\left(\frac{1}{\mathrm{Re}Da} + \frac{Fs}{Da}|\mathbf{u}|\right)\overline{\rho}w,\end{aligned} \tag{7}$$

$$\overline{\rho c}_p \frac{\partial \Theta}{\partial t} + \frac{1}{r}\frac{\partial}{\partial r}(r\overline{\rho}u\Theta) + \frac{\partial}{\partial z}(\overline{\rho}w\Theta) = \frac{1}{\mathrm{Pr}}\overline{k}\left[\frac{1}{r}\frac{\partial}{\partial r}\left(r\frac{\partial \Theta}{\partial r}\right) + \frac{\partial}{\partial z}\left(\frac{\partial \Theta}{\partial z}\right)\right], \tag{8}$$

$$\overline{\rho}\frac{\partial c}{\partial t} + \frac{1}{r}\frac{\partial}{\partial r}(r\overline{\rho}uc) + \frac{\partial}{\partial z}(\overline{\rho}wc) = \frac{1}{Sc}\overline{D}\left[\frac{1}{r}\frac{\partial}{\partial r}\left(r\frac{\partial c}{\partial r}\right) + \frac{\partial}{\partial z}\left(\frac{\partial c}{\partial z}\right)\right], \tag{9}$$

where $\overline{\rho} = \rho_e/\rho_f$, $\overline{\mu} = \mu_e/\mu_f$, $\overline{c}_p = c_{pe}/c_{pf}$, $\overline{k} = k_e/k_f$, $\overline{D} = D_e/D_f$.

3. Results and discussion

The ammonothermal growth system with a forward solubility is considered in which case the charge is put below the baffle. Fig. 2 shows the temperature distribution in the research-grade autoclave with an internal diameter of 2.22 cm. The temperature gradients across the baffle are large which

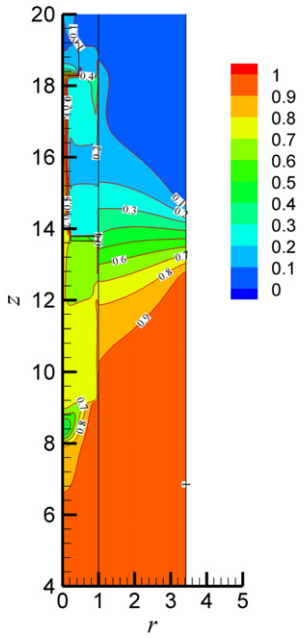

Fig. 2. Temperature field in an ammonothermal system with a baffle opening of 10% in the cross-sectional area (central opening of 5% and ring opening of 5%).

may cause depositions of GaN near the baffle. The baffle opening is selected to achieve a certain temperature difference across the baffle, and thus certain supersaturation in the growth zone of the autoclave and growth rate of crystals can be achieved. The upward flow in the central hole can bring hot solvent toward the bottom of the seed (Fig. 3). The flow strength in the fluid layer depends on the Grashof number, which is proportional to the temperature difference on the sidewall and the cube of the internal radius of the autoclave. Flow in the charge layer depends on the modified Grashof number, i.e., the product of Grashof number and Darcy number, which is proportional to the square of the average diameter of particles. The flow strength in the porous layer can be increased by increasing the size of particles, or by putting particles in bundles as in the hydrothermal growth. Reducing the baffle opening can reduce the overall flow strength in the fluid region and the volumetric flow rate through the central hole of the baffle.

The concentration field is shown in Fig. 4. The constraints for the ammonothermal growth include dissolving of charge, nucleation on the sidewall, transfer of nutrient from charge to seed, and growth kinetics. Since the dimensionless temperature under the seed is higher than the dimensionless concentration, there will be dissolving of the seed there. The temperature decreases suddenly from the bottom of the seed to the side of the seed, deposition will occur on the side and top of the seed. The mass transfer between the dissolving zone and the growth zone is important for the continued growth of GaN crystals. From the calculation, the total deposit rate including deposition on sidewalls is about 9 g/day, and the growth rate is about 1 mm/day if the mass transfer coefficient for crystal growth is taken as 10^{-6} m/s and the charge particle size is of 1 mm. For the particle size of 1 mm, the dimensionless concentration inside the autoclave is much less than 1, and the low supersaturation in the growth zone can reduce depositions on the baffle and the sidewall of the autoclave.

Figs. 5–7 show the evolving of average flow velocity in the center hole and the ring gap for different baffle openings. For the case of baffle opening of 10% in the cross-sectional area (center opening of 5% and ring opening of 5%), the average velocity in the central hole is about 0.02 m/s, while the average velocity in the ring gap is about −0.02 m/s. The fluctuation of velocity in central hole is lager than that in the ring gap.

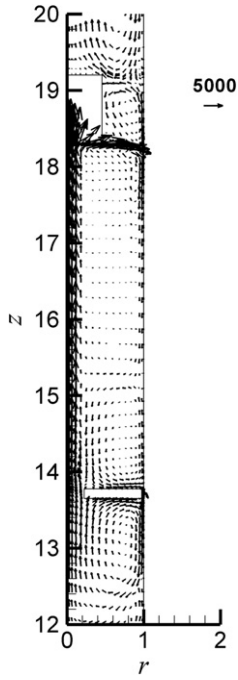

Fig. 3. Fluid flow in a system with a baffle opening of 10%.

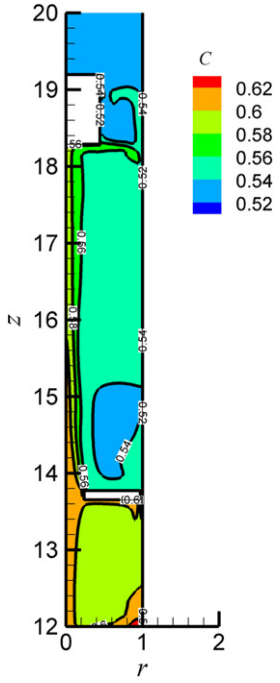

Fig. 4. Concentration field in a system with a baffle opening of 10%.

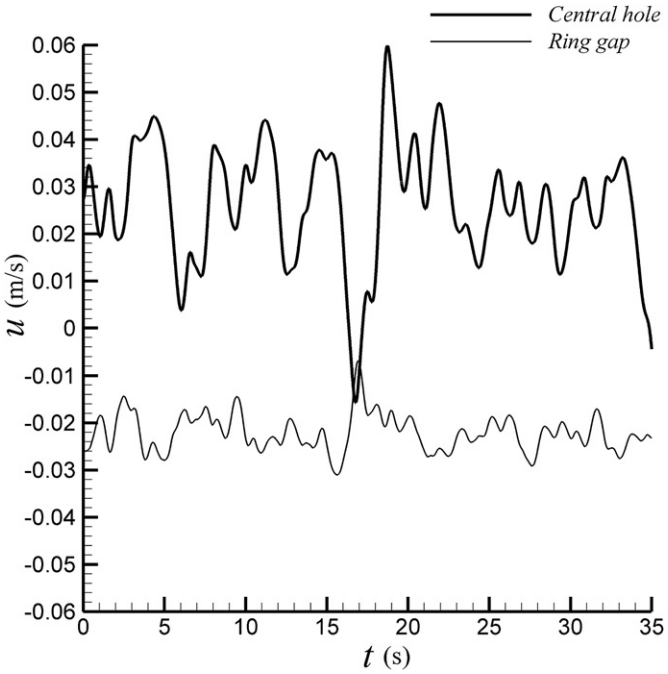

Fig. 5. Average velocity in the central hole and ring gap for the baffle opening of 10%.

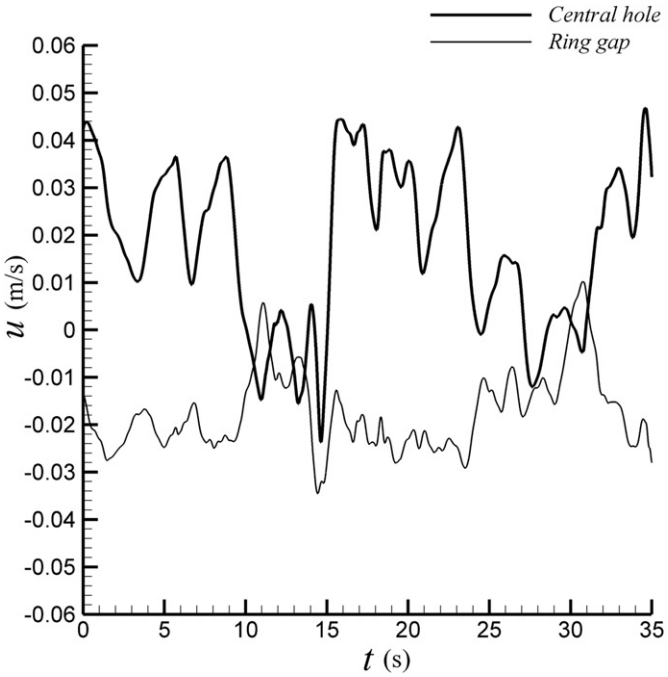

Fig. 6. Average velocity in the central hole and ring gap for the baffle opening of 15%.

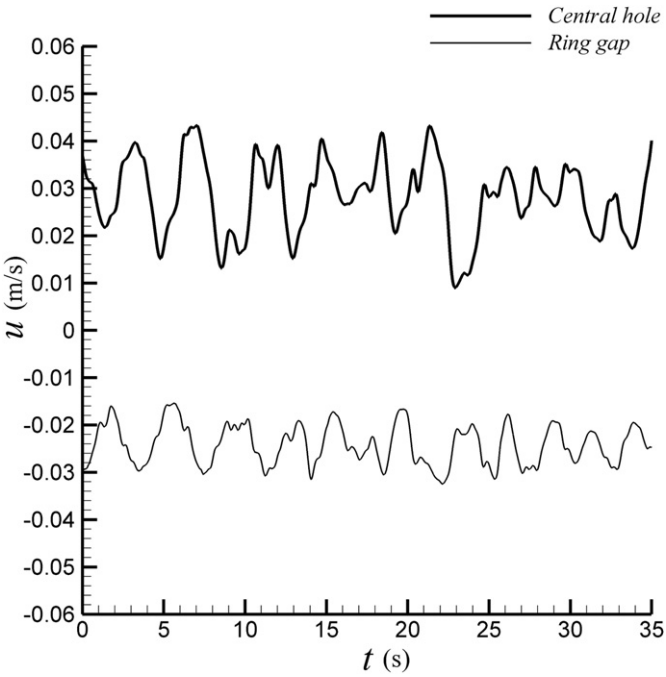

Fig. 7. Average velocity in the central hole and ring gap for the baffle opening of 20%.

For 70% fill, the density of the ammonia under supercritical conditions is about 476 kg/m^3 while the density of the ammonia before filling is taken as 681 kg/m^3 at -33 °C [9]. From the calculation, the average volumetric flow rate is about 4×10^{-7} m^3/s, and the transport rate of nutrient through the central hole of the baffle is about 0.49 kg/day if solubility is taken as 3% in weight. So the constraint for continued growth of GaN is the growth kinetics and the total area of seed surfaces in the case of 10% baffle opening.

For the case of baffle opening of 15% in the cross-sectional area (center opening of 10% and ring opening of 5%), the flow is highly oscillatory since the central hole and the ring gap have unequal areas (Fig. 6). The average velocity is about 0.02 m/s in the central hole and the average velocity is about -0.02 m/s in the ring gap. The average volumetric flow rate is about 4×10^{-7} m^3/s. For the case of baffle opening of 20% in the cross-sectional area (center opening of 10% and ring opening of 10%), the velocity in the central hole is positive for the most time, while that in ring gap is negative (Fig. 7), and the fluid flow across the baffle is a cyclic flow. The average velocity is about 0.025 m/s in the central hole and the average velocity is about -0.025 m/s in the gap ring. The volumetric flow rate of the solvent is about 1.2×10^{-6} m^3/s in the central hole.

The transport phenomena in a large-size system with an internal diameter of 4.44 cm are studied. In order to investigate the effect of baffle opening on the growth process, we consider here baffle openings of 8%, 12%, 16% and 20%, and assume that the center opening and the ring opening have the same area. Fig. 8 shows the volumetric flow rates in the central hole and the ring gap. It can be seen that, for the baffle opening of 8%, the volumetric flow rate in the center hole is about 4×10^{-6} m^3/s. The fluctuating amplitude of the volumetric flow rate in the central hole is much larger than that in the ring gap. In this case, the fluid flow is an oscillatory flow in the high-pressure autoclave. An oscillatory flow is adverse to the GaN crystal growth process because raw materials cannot be transported efficiently to the vicinity of the seeds. In the cases of 12%, 16% and 20% openings, the volumetric flow rate in the central hole increases with the baffle opening, and the average flow velocity is negative in the center hole. The fluid flow across the baffle is an anticlockwise circulating flow, which is in favor of the transfer of raw material.

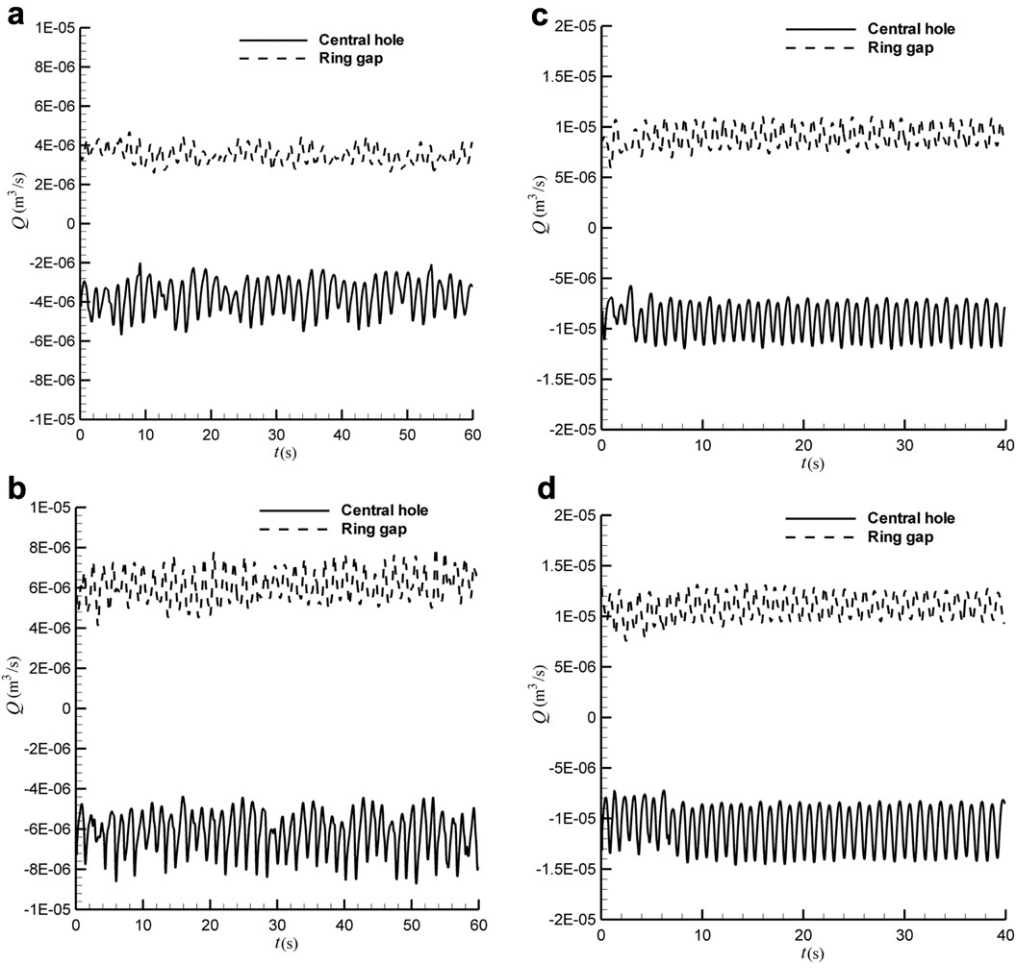

Fig. 8. Volumetric flow rate in the autoclave with an internal diameter of 4.44 cm and baffle openings of (a) 8%, (b) 12%, (c) 16% and (d) 20%.

The effect of the internal diameter of autoclave on the mass transport is also investigated. Figs. 9and 10 show the evolving of average flow velocity in the center hole and the ring gap for systems with different inner diameters. For the system with an inner diameter of 4.44 cm and baffle opening of 10% in the cross-sectional area (center opening of 5% and ring opening of 5%), the flow across the baffle is an anticlockwise circulating flow (Fig. 9). The average velocity is about −0.05 m/s in the central hole and the average velocity is about 0.05 m/s in the ring gap. The average volumetric flow rate is about 4.4×10^{-6} m^3/s. When the inner diameter increases from 2.22 cm to 4.44 cm, the volumetric flow rate through the central hole increases almost 9 times. For the system with an inner diameter of 10 cm and baffle opening of 10% in the cross-sectional area (center opening of 5% and ring opening of 5%), the fluid flow across the baffle is also an anticlockwise circulating flow. The average velocity is about −0.06 m/s in the central hole and the average velocity is about 0.06 m/s in the gap ring (Fig. 10). The volumetric flow rate of the solvent is about 2.5×10^{-5} m^3/s in the central hole. The volumetric flow rate though the central hole in the system with an inner diameter of 10 cm increases 60 times compared with that in the system with an inner diameter of 2.22 cm.

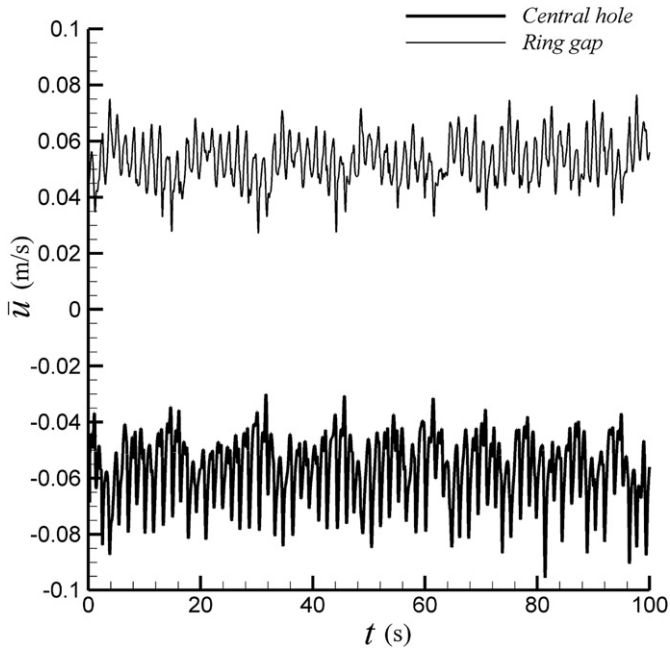

Fig. 9. Average velocity in the central hole and ring gap in the system with an inner diameter of 4.44 cm and baffle opening of 10%.

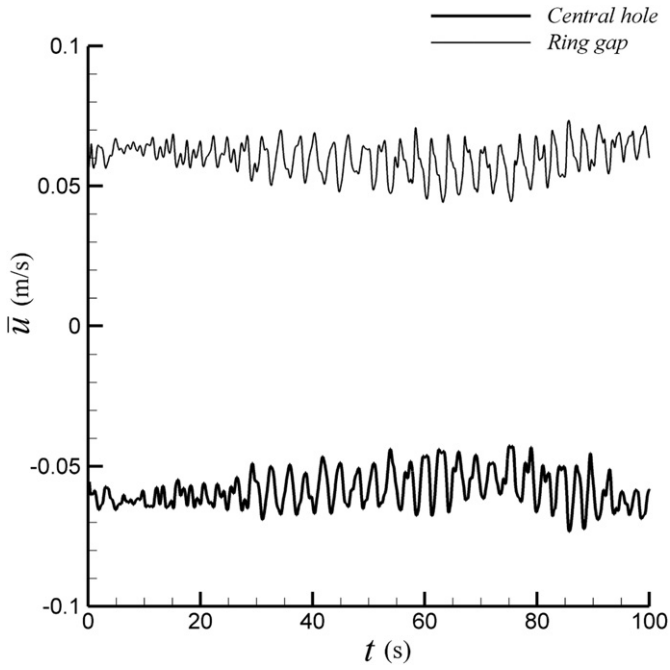

Fig. 10. Average velocity in the central hole and ring gap in the system with an inner diameter of 10 cm and baffle opening of 10%.

4. Conclusions

Heat and mass transfer in the ammonothermal growth systems with a forward solubility was modeled. For the research-grade system with an internal diameter of 2.22 cm, the temperature gradients across the baffle are large which may cause some depositions of GaN near the baffle. The baffle opening is selected to achieve a certain temperature difference across the baffle, and thus certain supersaturation in the growth zone of the autoclave. The effects of the baffle opening on the flow pattern and the reagent transport have been studied. For the baffle opening of 10%, the fluid flow around the baffle is a clockwise circulating flow, and goes upward in the central hole, downward through the ring gap. The constraint for continued growth of GaN is the growth kinetics and the total area of the seed surfaces. For the baffle opening of 15%, the flow is highly oscillatory since the central hole and the ring gap have unequal areas. For the baffle opening of 20%, the flow around the baffle is also a clockwise circulating flow. For the charge particle size of 1 mm, the low supersaturation in the growth zone can reduce depositions on the baffle and the sidewall of the autoclave.

Transport phenomena have been also studied in large-size ammonothermal systems. For the autoclave with an internal diameter of 4.44 cm, the baffle opening is an important parameter for transport of nutrient. When the baffle opening increases from 8% to 12%, the flow pattern changes from an oscillatory flow to a steady circulating flow. In the case of 12% opening, the flow in the autoclave exhibits a steady circulation; hence the growth is stable. The transfer of raw material depends on the baffle opening and the temperature difference between growth zone and dissolving zone. For the autoclave with an internal diameter of 10 cm and a 10% baffle opening, flow pattern across the baffle is an anticlockwise circulation.

Acknowledgments

The project supported by the National Science Foundation of China (10972226, 50776098).

References

[1] T. Hashimoto, K. Fujito, M. Saito, J.S. Speck, S. Nakamura, Japanese Journal of Applied Physics 44 (2005) L1570–L1572.
[2] T. Hashimoto, K. Fujito, B.A. Haskell, P.T. Fini, J.S. Speck, S. Nakamura, Journal of Crystal Growth 275 (2005) e525–e530.
[3] T. Hashimoto, M. Saito, K. Fujito, F. Wu, J.S. Speck, S. Nakamura, Journal of Crystal Growth 305 (2007) 311–316.
[4] M.P. D'Evelyn, H.C. Hong, D.-S. Park, H. Lu, E. Kaminsky, R.R. Melkote, P. Perlin, M. Lesczynski, S. Porowski, R.J. Molnar, Journal of Crystal Growth 300 (2007) 11–16.
[5] M. Bockowski, P. Strak, I. Grzegory, B. Lucznik, S. Porowski, Journal of Crystal Growth 310 (2008) 3924–3933.
[6] D.R. Ketchum, J.W. Kolis, Journal of Crystal Growth 222 (2001) 431–434.
[7] M. Callahan, B.-G. Wang, K. Rakes, D. Bliss, L. Bouthillette, M. Suscavage, S.-Q. Wang, Journal of Materials Science 41 (2006) 1399–1407.
[8] B. Wang, M.J. Callahan, K.D. Rakes, L.O. Bouthillette, S.-Q. Wang, D.F. Bliss, J.W. Kolis, Journal of Crystal Growth 287 (2006) 376–380.
[9] B. Wang, M.J. Callahan, Journal of Crystal Growth 291 (2006) 455–460.
[10] M.J. Callahan, Q.-S. Chen, Hydrothermal and ammonothermal growth of ZnO and GaN, in: G. Dhanaraj, K. Byrappa, V. Prasad, M. Dudley (Eds.), Springer Handbook of Crystal Growth, Springer-Verlag, Berlin, 2010, pp. 655–689.
[11] R. Dwilinski, R. Doradzinski, J. Garczynski, L. Sierzputowski, M. Palczewska, A. Wysmolek, M. Kaminska, MRS Journal of Nitride Semiconductor Research 3 (1998) 25.
[12] R. Dwilinki, R. Doradzinski, J. Garczynski, L.P. Sierzputowski, A. Puchalski, Y. Kanbara, K. Yagi, H. Minakuchi, H. Hayashi, Journal of Crystal Growth 310 (2008) 3911–3916.
[13] R. Dwilinski, R. Doradzinski, J. Garczynski, L.P. Sierzputowski, A. Puchalski, Y. Kanbara, K. Yagi, H. Minakuchi, H. Hayashi, Journal of Crystal Growth 311 (2009) 3015–3018.
[14] A. Yoshikawa, E. Ohshima, T. Fukuda, H. Tsuji, K. Oshima, Journal of Crystal Growth 260 (2004) 67–72.
[15] Y. Kagamitani, D. Ehrentraut, A. Yoshikawa, N. Hoshino, T. Fukuda, S. Kawabata, K. Inaba, Japanese Journal of Applied Physics 45 (5A) (2006) 4018–4020.
[16] D. Ehrentraut, N. Hoshino, Y. Kagamitani, A. Yoshikawa, T. Fukuda, H. Itoh, S. Kawabata, Journal of Materials Chemistry 17 (2007) 886.
[17] T. Fukuda, D. Ehrentraut, Journal of Crystal Growth 305 (2007) 304–310.
[18] D. Ehrentraut, Y. Kagamitani, C. Yokoyama, T. Fukuda, Journal of Crystal Growth 310 (2008) 891–895.
[19] K. Fujii, G. Fujimoto, T. Goto, T. Yao, Y. Kagamitani, N. Hoshino, D. Ehrentraut, T. Fukuda, Journal of Crystal Growth 310 (2008) 896–899.
[20] D. Ehrentraut, Y. Kagamitani, T. Fukuda, F. Orito, S. Kawabata, K. Katano, S. Terada, Journal of Crystal Growth 310 (2008) 3902–3906.
[21] T. Hashimoto, F. Wu, James S. Speck, S. Nakamura, Nature Materials 6 (2007) 568–571.

[22] Q.-S. Chen, V. Prasad, W.R. Hu, Journal of Crystal Growth 258 (2003) 181–187.
[23] Q.-S. Chen, S. Pendurti, V. Prasad, Journal of Crystal Growth 266 (2004) 271–277.
[24] Q.-S. Chen, S. Pendurti, V. Prasad, Journal of Materials Science 41 (2006) 1409–1414.
[25] M. Carr, Journal of Fluid Mechanics 509 (2004) 305–329.
[26] V. Prasad, Convective flow interaction and heat transfer between fluid and porous layers, in: S. Kakaç, et al. (Eds.), Convective Heat and Mass Transfer in Porous Media, Kluwer, Netherlands, 1991, pp. 563–615.

Qi-Sheng Chen graduated and obtained the MS degree both at Department of Mechanics, Peking University and received the PhD degree from Institute of Mechanics, Chinese Academy of Sciences in 1997. Chen was Faculty administrator and coordinator at Department of Mechanical Engineering, Florida International University in 2001. Since 2002, Chen has been research professor at Institute of Mechanics, Chinese Academy of Sciences. Research activities include microgravity fluid mechanics and crystal growth modeling.

Jun-Yi Yan graduated at Institute of Mechanics, Chinese Academy of Sciences in 2012. His research field is about numerical simulation and optimization study in the PVT growth process of SiC crystals.

Yan-Ni Jiang obtained Ph. D. degree from Institute of Mechanics, Chinese Academy of Sciences in 2011. Her research field is about GaN crystal growth by the ammonothermal method.

Wei Li graduated at Institute of Mechanics, Chinese Academy of Sciences in 2011. His research field is about numerical study on the reciprocating compressible flow in thermoacoustic refrigeration.